INTERNATIONAL JOURNAL OF INTEGRATED ENGINEERING
ISSN: 2229-838X e-ISSN: 2600-7916

IJIE

Vol. 17 No. 1 (2025) 401-415
https://publisher.uthm.edu.my/ojs/index.php/ijie

Optimizing Control Strategies for Hand Exoskeleton: A Comparative Study of Controllers

Ab Wafi Ab Aziz[1,3], Jamaludin Jalani[2]*, Amirul Syafiq Sadun[1]

[1] *Department of Electrical Engineering Technology, Faculty of Engineering Technology Universiti Tun Hussein Onn Malaysia, Pagoh Campus, Hab Pendidikan Tinggi Pagoh, M 1, Jalan Panchor, 84600 Panchor, Johor, MALAYSIA*
[2] *Department of Electrical and Electronic Engineering, Faculty of Electrical and Electronic Engineering Universiti Tun Hussein Onn Malaysia, Parit Raja, 86400 Batu Pahat, Johor, MALAYSIA*
[3] *Department of Electrical Engineering Technology, Faculty of Electrical Technology and Engineering Universiti Teknikal Malaysia Melaka, Hang Tuah Jaya, 76100 Durian Tunggal, Melaka, MALAYSIA*

*Corresponding Author: jamalj@uthm.edu.my
DOI: https://doi.org/10.30880/ijie.2025.17.01.033

Article Info

Received: 31 October 2024
Accepted: 9 January 2025
Available online: 30 April 2025

Keywords

Hand exoskeletons, hand impairment, stroke patients, sliding mode control, comparative analysis, controller performance, assistive devices

Abstract

This study presents a comparative analysis of three controllers (PI, Fuzzy Logic Control, and Sliding Mode Control) for hand exoskeletons designed for stroke patients. The research evaluates the controllers' performance in manipulating the exoskeleton to specific target angles, with results indicating competitive performance across various data metrics. The methodology involves the design and simulation of each controller using Matlab Simulink software, with the hand exoskeleton featuring a unique four-finger rigid design and an Actuonix linear motor. Notably, the study identifies Sliding Mode Control as the most effective controller, demonstrating superior stability, accuracy, minimal overshoot, zero steady-state error, and the fastest settling time. This research significantly advances hand exoskeleton technology for individuals with hand impairments. The study offers valuable insights for the development and implementation of control systems in hand exoskeleton technology, with implications for assistive applications.

1. Introduction

Hand exoskeletons: wearable devices that are designed to apply active force to the user's fingers through mechanical components; serve various purposes and applications. This device can be broadly categorized into assistive technology, rehabilitation systems, augmentation exoskeletons, and haptic feedback mechanisms [1]–[5]. Assistive devices are intended to replace impaired hand functioning, while rehabilitation systems focus on restoring functionality lost due to injury or medical conditions [6], [7]. Augmentation exoskeletons enhance grasping abilities beyond normal levels and haptic hand exoskeleton devices are applied in teleoperation or virtual reality haptic systems [8]–[10]. Specifically for individuals facing hand impairments, these devices can significantly enhance their quality of life by facilitating activities of daily living (ADLs) and aiding in rehabilitation [11]–[16]. These impairments commonly stem from neurological conditions like stroke or musculoskeletal disorders.

Moreover, achieving precise position control in hand exoskeletons requires the integration of sensors, algorithms, actuators, and feedback mechanisms to accurately manage and support the position of the user's hand and fingers. Sensors detect the hand's position and movement, with data processed by onboard electronics or a connected computer system. Control algorithms interpret this data, calculating the necessary forces or constraints

required to achieve the desired hand position based on user intent and task requirements. Movement mechanism; including an actuator, then apply these forces to the user's hand. Throughout this process, feedback loops ensure accuracy, with sensory feedback provided to the user and adjustments made based on sensor feedback to continuously refine position control. This capability enables tasks such as object manipulation, fine motor skill execution, assistance for individuals with hand impairments, finding applications in rehabilitation, assistive technology, and precise industrial tasks.

As research on hand exoskeletons has significantly expanded, identifying the optimal controller for position control has emerged as a crucial phase in hand exoskeleton development. Selecting the most suitable controller for a particular hand exoskeleton is paramount to ensure precise movement to various angular positions according to the user's preferences. This requires considering some factors such as responsiveness, accuracy, and compatibility with the exoskeleton's design and intended applications. Various controllers are being used by the researchers for their designed hand exoskeleton. Dario Marconi et al. [17] and Alberto Topini et al. [18] have utilized conventional Proportional-Integral-Derivative (PID) control in their designs. In the HandeXos-Beta exoskeleton, Dario Marconi et al. [17] achieved suitable position control performance using PID control with step input. Alberto Topini et al. [18] applied PID control to manage individual finger movement in their hand exoskeleton. Meanwhile, Cruz-Sanchez et al. [19] implemented a more advanced controller for their electromyography (EMG) controlled hand exoskeleton, which featured 8 degrees of freedom (DOF). Results indicated that the controller was able to trajectory-track the reference position with minimal error. Moreover, several control strategies have been explored to achieve accurate control of finger positions and forces, aiming for human-like ability [20]. Model-based control has been utilized to achieve desired finger position and forces with multi-degree-of-freedom exoskeletons, demonstrating superior performance compared to conventional control methods [21]. PID controllers have been found to effectively control the position of the index finger in exoskeleton devices, with performance exceeding 90% accuracy [22].

Therefore, drawing inspiration from the above-mentioned project, this study provides a thorough comparative analysis of three different controllers: Proportional Integral (PI) Controller, Fuzzy Logic Control (FLC), and Sliding Mode Control (SMC). The comparison, summarized in Table 1, outlines the advantages and disadvantages of each controller. The objective is to assess their efficacy in precisely regulating the position of the user's fingers within hand exoskeletons. By evaluating these controllers comprehensively, this research seeks to identify the most suitable control strategy for achieving optimal performance and user experience in hand exoskeleton systems.

Table 1 *Comparison table between controllers* [23]–[27]

Controller	Advantages	Disadvantages
Proportional Integral (PI) Control	Simple implementation Effective for linear systems Good stability	Poor performance in nonlinear systems
Fuzzy Logic Control (FLC)	Handles nonlinearities well No need for a precise mathematical model Flexible and adaptive	Complex design Requires extensive tuning
Sliding Mode Control (SMC)	Robust against disturbances Handles nonlinearities Fast response	Chattering effect Complex design and implementation

2. Methodology

Fig. 1 (a) shows the hand exoskeleton employed in this comparative study, featuring a unique four-finger rigid design. Drawing inspiration from D. Esposito et al., [28] as shown in Fig. 1 (b), we enhanced the design by simplifying and refining its components. This included minimizing linkages using a curve flange and optimizing the attachment of the phalanges adapter to the user's fingers by eliminating the need for Velcro strips. This refined design not only simplifies reproduction for various users but also minimizes the need for extensive adjustments in linkage measurements to accommodate different hand sizes. By eliminating the use of Velcro strips, we significantly enhance the comfort of users wearing the hand exoskeleton. Actuating this innovative device is the Actuonix L12-30-100-6-R linear motor model, boasting a maximum speed of 13mm/s under no-load conditions,

Int. Journal of Integrated Engineering Vol. 17 No. 1 (2025) p. 401-415

a maximum force of 42N, and a stroke length of 30mm. An Arduino Uno is utilized through serial communication to facilitate communication between the hand exoskeleton and Matlab Simulink for position control.

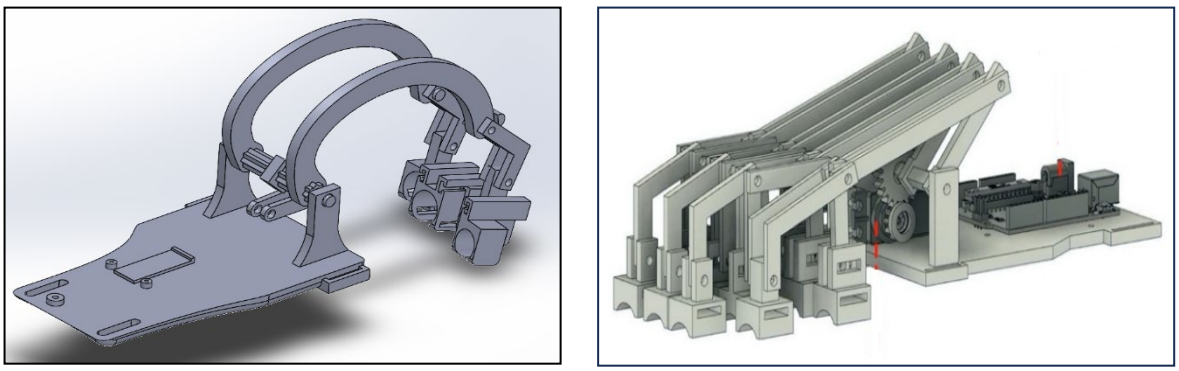

(a) **(b)**

Fig. 1 *Hand exoskeleton comparison (a) Used in this comparative study; (b) From [18]*

2.1 Controller Design and Simulation

It is essential to decide the optimum controller for the movement of the hand exoskeleton. In this comparative study, three distinct controllers are chosen which are the Proportional-Integral (PI) controller, Fuzzy Logic Control (FLC), and Sliding Mode Control (SMC). The PI controller was chosen because of its simplicity to implement and its well-known performance in various applications demanding continuous and precise control modulation. Meanwhile, FLC is chosen due to its capacity to manage imprecision and uncertainty through its rule-based system operation that mimics certain aspects of human reasoning [29]–[31]. The SMC was chosen because of its capability to handle disturbance which makes it well-known as a robust and resilient controller [32]–[34]. Matlab Simulink serves as the focal software for designing and implementing all three controllers governing the hand exoskeleton.

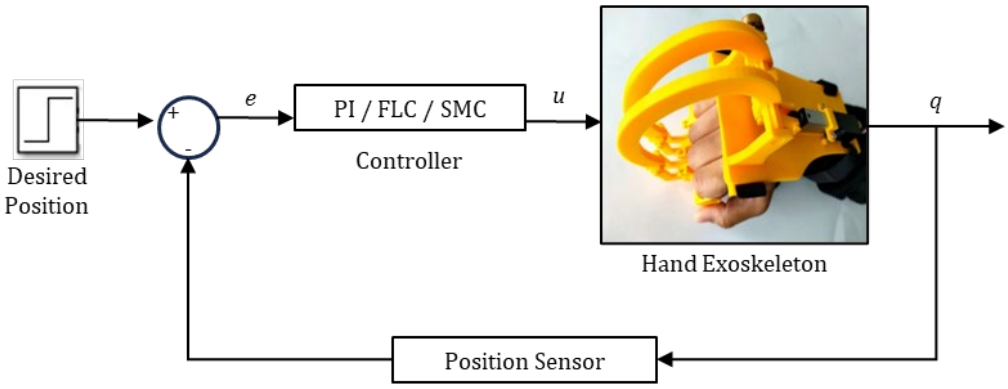

Fig. 2 *Block diagram for controller implementation*

In Fig. 2, the encompassing block diagram provides a comprehensive overview of the experimental setup, establishing a foundation for the performance analysis of each controller. The error (e) is delineated as the disparity between the actual angle position (q) of the hand exoskeleton, as detected by the position sensor, and the desired angle position. The controller computes the input signal (u) for the linear motor to rectify this error. Facilitating this communication loop, the Arduino Uno functions as the data acquisition (DAQ) transitional between Matlab Simulink and the hand exoskeleton, managing the transmission and reception of signals (u and q). This robust integration ensures a seamless exchange of information for precise control and analysis within the experimental framework.

2.1.1 PI Controller

The PID controller consists of three core components: Proportional, Integral, and Derivative, which can be used individually or in various combinations. The most common configurations include P, PI, PD, and PID control. The mathematical expression for a PID controller is given by:

$$u(t) = K_p e(t) + K_i 0 \int_0^t e(t)dt + K_d \frac{de(t)}{dt} \quad (1)$$

Here, K_p, K_i, and K_d represent the Proportional, Integral, and Derivative gains, respectively. The Proportional term provides immediate correction based on the present error, the Integral term addresses steady-state error by accumulating past errors, and the Derivative term predicts future error trends by evaluating the error's rate of change. In this study, a PI controller is employed, wherein the derivative component is excluded, simplifying Eq. (1) to:

$$u(t) = K_p e(t) + K_i 0 \int_0^t e(t)dt \quad (2)$$

The Derivative component has been omitted for controlling the position of the hand exoskeleton due to its sensitivity to noise and rapid fluctuations in the signal, which can be detrimental in a system requiring smooth and precise movements. In applications like hand exoskeletons, where the control must accommodate subtle and continuous adjustments, the derivative action may introduce instability and unwanted oscillations. Therefore, the PI controller provides a more stable and reliable approach for this particular application.

The implementation of the PI controller is executed through the PID block within Matlab Simulink, as illuminated in Fig. 3. The Block Parameter interface for the PID controller block prominently features the controller type, with "PI" selected to characterize its operation. Tuning the controller is facilitated through the PID Tuner, accessed via the "Tune" button, where the dynamic adjustment of parameters is performed. The tuning process involves manipulating the sliders for "Response Time" and "Transient Behavior," strategically shifting them either to the right or left. The consequential impact of these adjustments is visually depicted in the preview outcome graph at the bottom of the PID Tuner interface. Our goal is to fine-tune the PI controller, ensuring an outcome without overshot, the fastest settling time, and minimal steady-state error. Fig. 4 provides a visual representation of the PID Tuner interface, offering insights into the meticulous tuning process applied to optimize the performance of the PI controller.

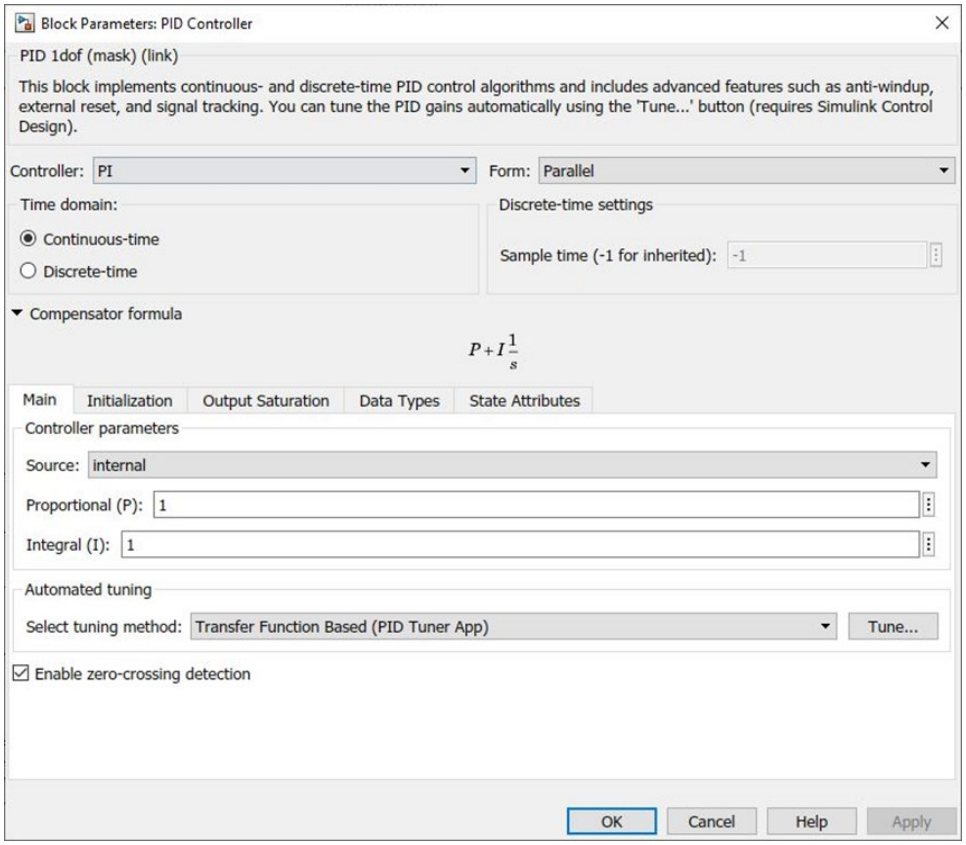

Fig. 3 *Block parameter interface for PID controller in Matlab Simulink*

Int. Journal of Integrated Engineering Vol. 17 No. 1 (2025) p. 401-415

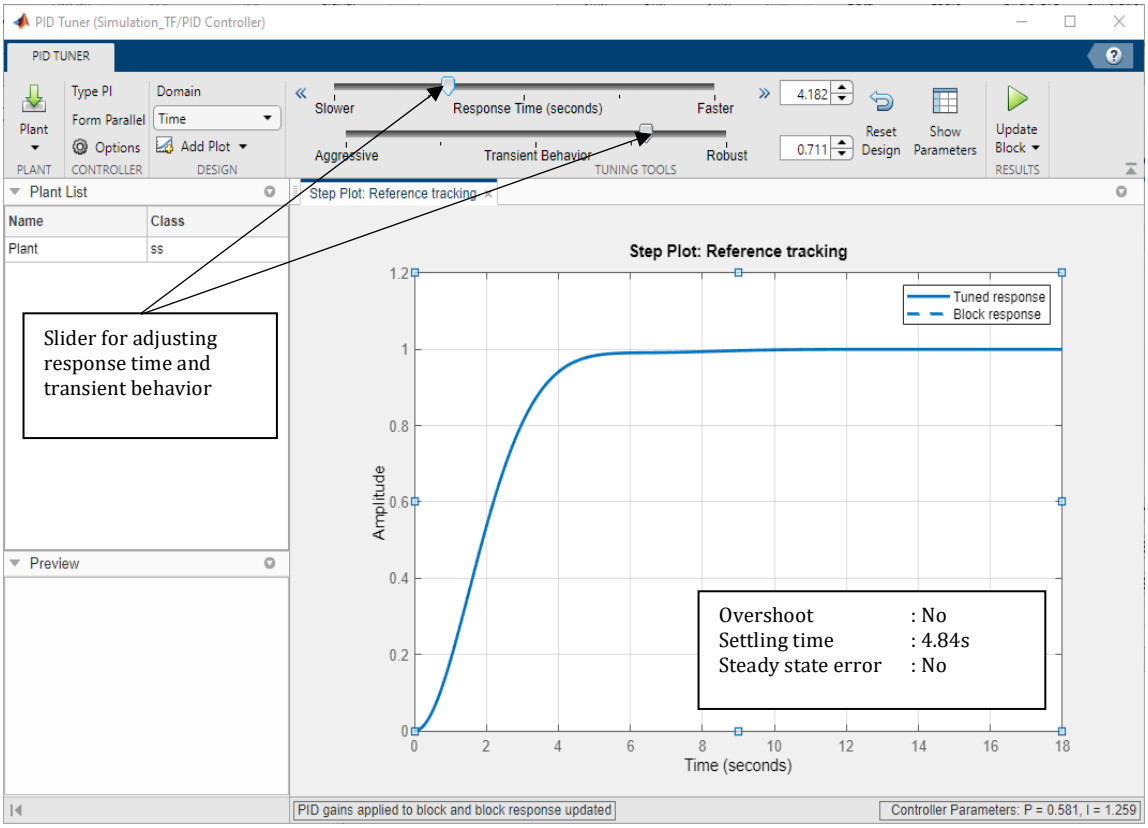

Fig. 4 *PID tuner interface*

2.1.2 Fuzzy Logic Control (FLC)

The design and implementation of the Fuzzy Logic Controller (FLC) for regulating the angular position of a hand exoskeleton are coordinated through the Fuzzy Logic Toolbox integrated into the Matlab software environment. Accessible via the command "fuzzyLogicDesigner" in Matlab's Command Window, the Fuzzy Logic Designer interface, shown in Fig. 5, provides a user-friendly platform for configuring the FLC parameters. In this setup, two input variables are selected: the error, $e(t)$, representing the deviation of the current position, $y(t)$ from the desired position, $r(t)$, as outlined in Eq. (3), and the error rate $\Delta e(t)$, denoting the rate of change of the error over time as shown in Eq. (4). These variables are carefully bounded within the ranges of -67° to 67° for the error and -120 to 120 for the error rate, ensuring compatibility with the exoskeleton's operational requirements.

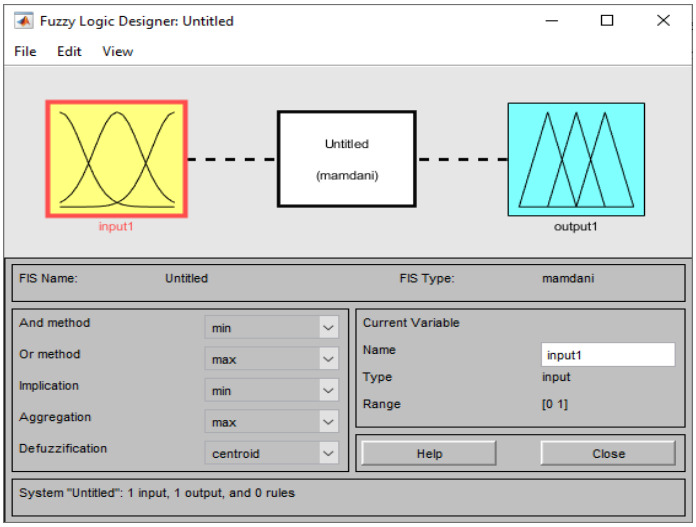

Fig. 5 *Fuzzy logic designer interface*

$$e(t) = r(t) - y(t) \tag{3}$$

$$\Delta e(t) = e(t) - e(t-1) \tag{4}$$

The output variable, torque $T(t)$, drives the movement of the exoskeleton The torque is determined by aggregating the results of all relevant rules using the Mamdani inference method, where each rule's contribution is computed as the minimum of the membership functions for $e(t)$ and $\Delta e(t)$. The final output $T(t)$ is derived through defuzzification using the centroid method [35], as shown in Eq. (5), where $u_i(z_i)$ is the membership value of the output for rule *i*, and z_i is the corresponding output value of rule *i*. This computed torque is then applied to adjust the exoskeleton's actuator, thereby modifying the position $y(t+1)$, as described in Eq. (6). With a torque output range from -5 to 5, the FLC provides precise control in response to variations in the input variables.

To enhance control effectiveness, the FLC design incorporates five distinct fuzzy subsets: Negative Big (NB), Negative Small (NS), Zero (Z), Positive Small (PS), and Positive Big (PB). Each subset represents a specific range of input or output values and plays a critical role in the controller's decision-making process.

$$T(t) = \frac{\sum_i u_i(z_i) \,.\, z_i}{\sum_i u_i(z_i)} \tag{5}$$

$$y(t+1) = y(t) + T(t) \tag{6}$$

Central to the FLC's functionality is the utilization of Gaussian membership functions, which define the degree of membership of input and output variables to each fuzzy subset. These functions provide a smooth and continuous transition between subsets, allowing for seamless control action across the entire operational range. The graphical representations showcased in Fig. 6 illustrate the membership functions for both input and output variables, offering a visual insight into the fuzzy subsets' boundaries and their corresponding degrees of membership. This strategic design approach not only ensures robust performance but also facilitates adaptability to varying operating conditions and precise manipulation of the exoskeleton's angular position. The integration of FLC within Matlab's environment empowers users with powerful tools for designing and fine-tuning control systems, paving the way for advanced applications in robotics and automation.

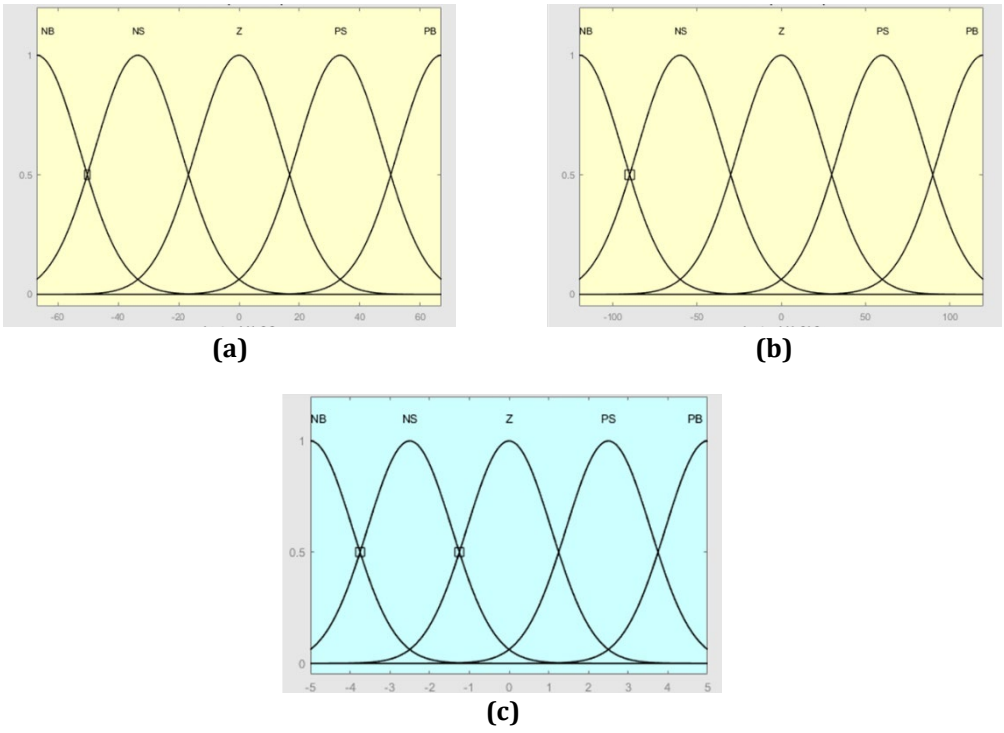

Fig. 6 *Membership function: (a) Input error, e; (b) Input error rate, de; (c) Output torque, u*

Int. Journal of Integrated Engineering Vol. 17 No. 1 (2025) p. 401-415

The rule base dictating the Fuzzy Logic Controller's (FLC) operation for governing the angular position of the hand exoskeleton is meticulously crafted through the formulation of IF–Then rules. These rules are carefully derived from a synthesis of insights gleaned from seminal works by B. Beraoui et al., [36] and P. Mitra et al., [37] alongside our team's extensive testing and experiential knowledge of the hand exoskeleton. A comprehensive summary of these rules, totaling 25 in number, is presented in Table 2. This table serves as a structured overview of the rule base, summarizing the conditions and corresponding actions guiding the FLC's decision-making process. Subsequently, these rules are seamlessly integrated into the Matlab Simulink environment using the intuitive Rule Editor interface, as exemplified in Fig. 7(a). Additionally, the Rule Viewer functionality, showcased in Fig. 7(b), enables simulation and visualization of the outcomes generated by these rules, facilitating a deeper understanding of their efficacy in governing the hand exoskeleton's angular position with precision and adaptability.

Table 2 *25 fuzzy rules*

Torque, *u*		Error rate, *de*				
		NB	NS	Z	PS	PB
Error, *e*	NB	NB	NB	NS	NS	Z
	NS	NB	NS	NS	Z	PS
	Z	Z	Z	Z	Z	Z
	PS	NS	Z	PS	PS	PB
	PB	Z	PS	PS	PB	PB

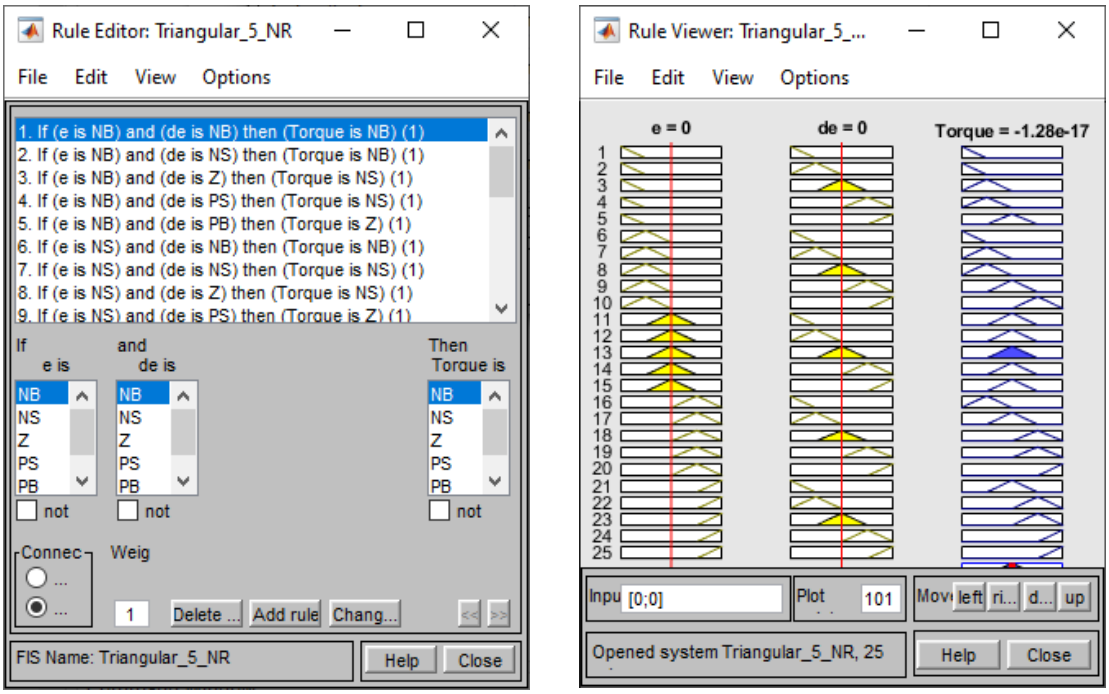

(a) **(b)**

Fig. 7 *Guidelines for conditions and corresponding actions of the FLC's decision-making process: (a) Rule editor interface; (b) Rule viewer interface*

2.1.3 Sliding Mode Control (SMC)

The Sliding Mode Control (SMC) is designed to drive the error (e) to zero as time (t) approaches infinity, specifically when the sliding surface, s = 0 [33], [38]. To realize this objective on our hand exoskeleton design, we define the sliding surface according to Eq. (7) [35]

$$s = \frac{de(t)}{dt} + Ce(t) \tag{7}$$

After defining the sliding surface, the subsequent step involves formulating a control signal capable of reaching and maintaining the sliding surface. Following the approach presented by J.M. Kiss et al., [33] and C.T. Chen et al., [38], the discontinuous controller output signal is derived using the sign function as expressed in Eq. (8).

$$\tau = K\, sgn\,(s) \tag{8}$$

In this equation, τ signifies the discontinuous torque control, and K is a positive constant. The utilization of the sign function induces a swift change in the control input, steering the system toward the sliding surface. While this abrupt change may lead to high-frequency oscillations, commonly known as chattering, it serves as a deliberate trade-off to achieve robustness and swift convergence during the reaching phase of SMC. However, chattering poses a potential risk to the motor, emphasizing the need to mitigate this phenomenon for the efficacy of SMC. A strategic approach to alleviate chattering involves substituting the sign function with the pseudo function, as depicted in Eq. (9), where δ serves as a tuning parameter to reduce chattering. The SMC controller is implemented in Matlab Simulink utilizing the block diagram, as illustrated in Fig. 8. This comprehensive design approach ensures the effectiveness of the SMC in guiding the hand exoskeleton with precision and adaptability, while simultaneously addressing the potential challenges associated with chattering, thereby enhancing the overall robustness and reliability of the control system.

$$\tau = K\left(\frac{s}{|s| + \delta}\right) \tag{9}$$

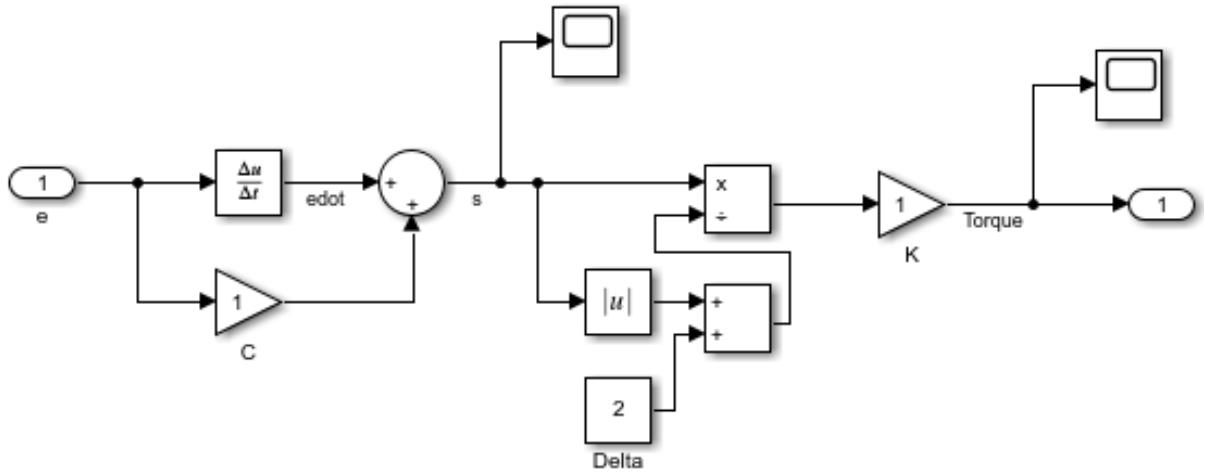

Fig. 8 *SMC Simulink block diagram*

3. Result and Discussions

Fig. 9 through Fig. 11 present the results of angular position control experiments conducted without the user wearing the hand exoskeleton, with target angles set at 60°, 40°, and 20°, respectively. In these figures, the blue solid line represents the output angle position for the PI controller, the green dotted line corresponds to the FLC output angle position, and the orange dash-dot line depicts the SMC output angle position. A clear trend emerges across all graphs: the PI controller exhibits the slowest overall trajectory in reaching the target position across all specified angles. Despite this, the PI controller demonstrates the quickest initial response for the 60° and 40° angles. At the one-second mark after the input signal initiation (t = 6s), the PI controller achieves 33° for the 60° target angle and 21° for the 40° target angle, outperforming both the FLC and SMC, which reach only 20° and 22° for the 60° target angle, and 17° and 19° for the 40° target angle, respectively.

However, as the response approaches the target angle, the PI controller's graph decelerates, making it the slowest to reach the final position. Notably, the PI controller's performance deteriorates as the target angle decreases, transitioning from the fastest initial response for 60° and 40° to the slowest initial response for the 20° target angle. In contrast, the FLC and SMC demonstrate more consistent performance across varying target angles, with minimal variation in response time as the target angle decreases.

Moreover, upon reaching a steady state, the PI controller's graph exhibits noticeable ripples across all target angles, particularly pronounced at the 20° target. These residual oscillations indicate a persistent steady-state error, which could negatively impact the long-term accuracy and stability of the exoskeleton's positioning. Conversely, the FLC and SMC graphs display no steady-state error, maintaining the desired position with high

Int. Journal of Integrated Engineering Vol. 17 No. 1 (2025) p. 401-415

precision, a critical attribute for applications demanding sustained accuracy, such as repetitive tasks or prolonged exoskeleton usage.

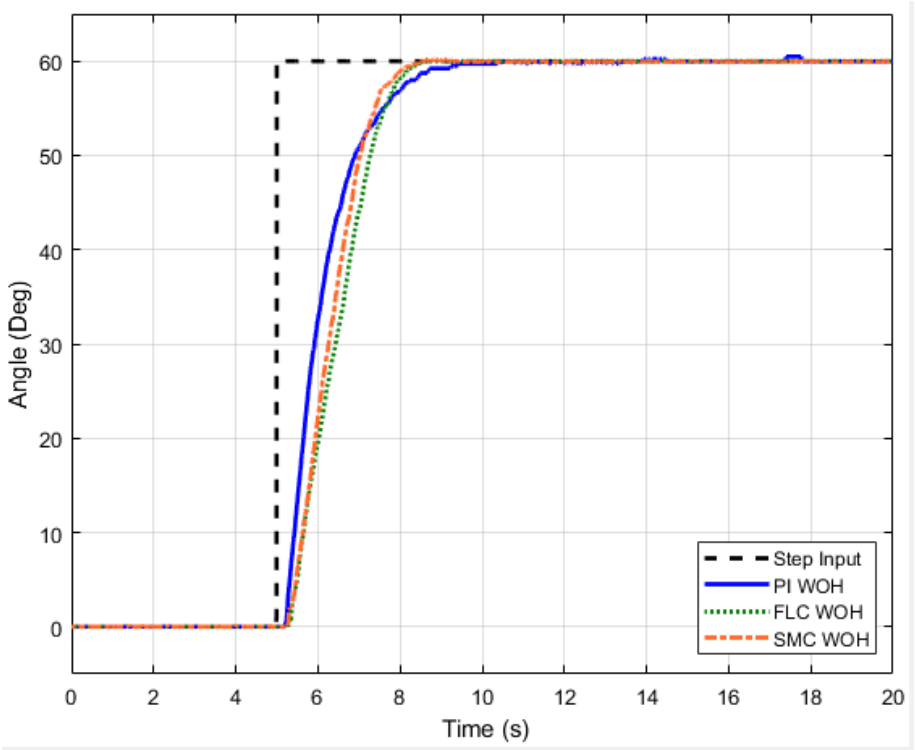

Fig. 9 *Graph output position for target angle 60° without the user's hand*

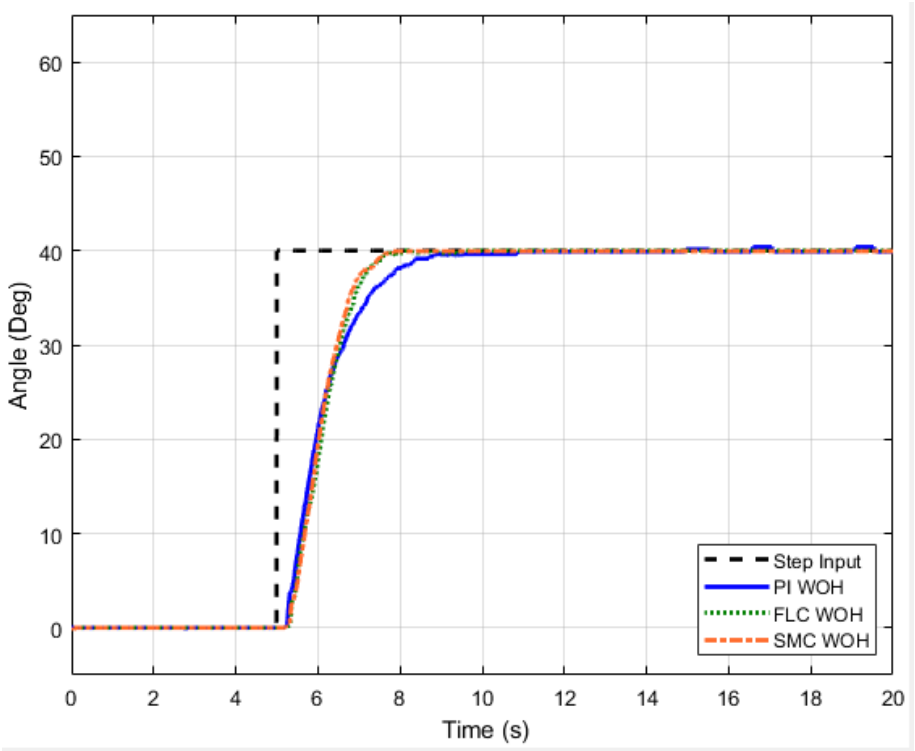

Fig. 10 *Graph output position for target angle 40° without the user's hand*

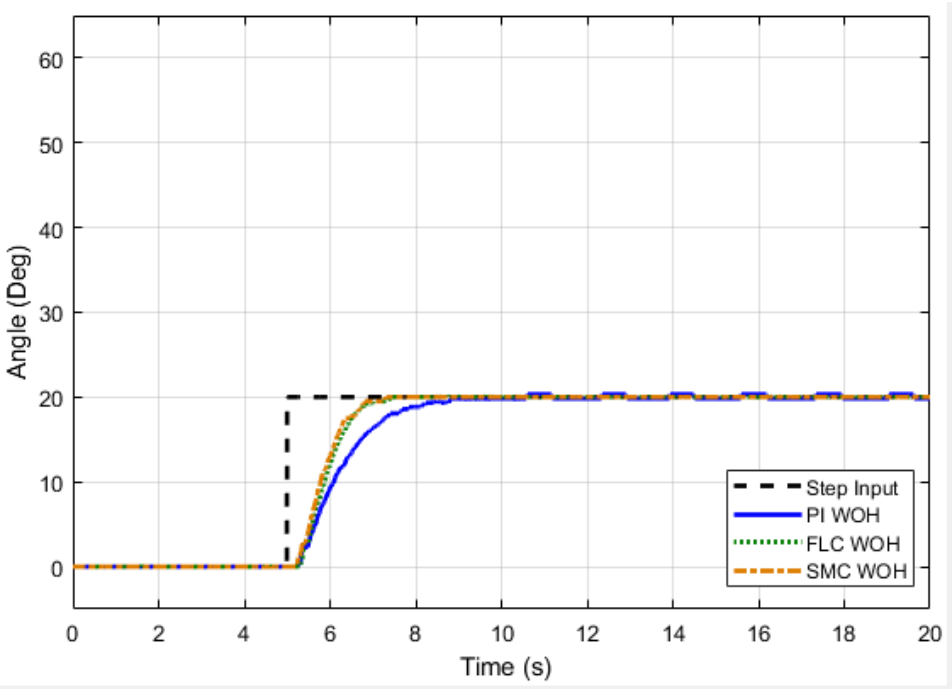

Fig. 11 *Graph output position for target angle 20° without the user's hand*

The FLC and SMC responses appear quite similar, particularly at the 40° and 20° target angles, where their graphs closely align for most of the time. However, a distinct difference emerges at the 60° target angle, where the SMC demonstrates a significantly faster response compared to the FLC. This suggests that while the FLC is effective, the SMC is superior in achieving rapid and precise control, especially at higher target angles. In conclusion, for conditions without the user's hand, the SMC outperforms the other two controllers, offering the fastest response in reaching the target angle with zero steady-state error. This superior performance highlights the SMC's robustness and suitability for applications requiring high-speed and accurate position control in hand exoskeleton systems.

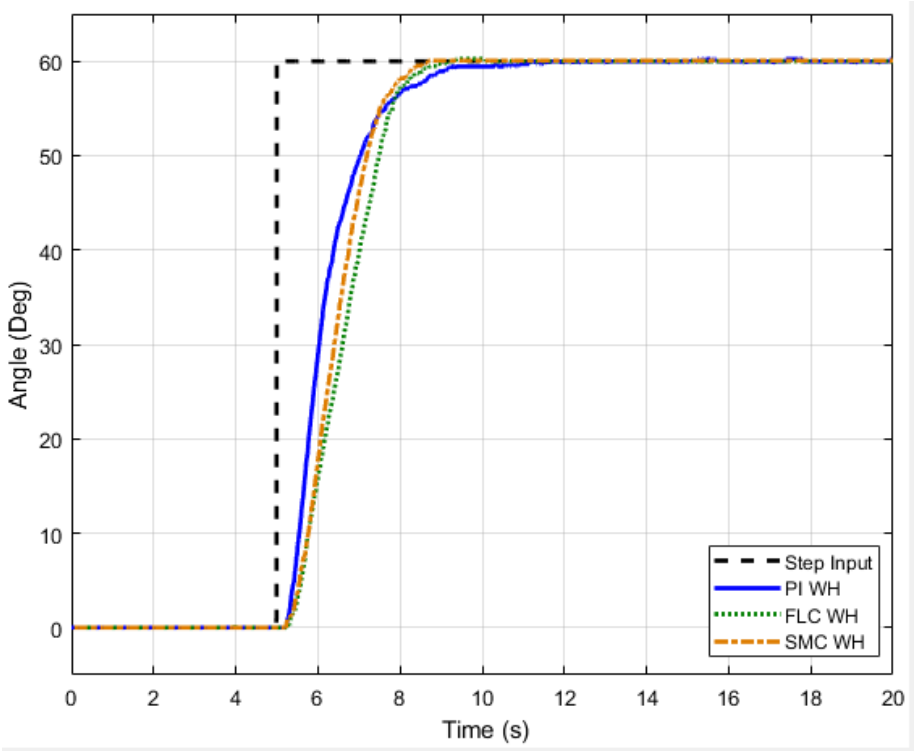

Fig. 12 *Graph output position for target angle 60° with the user's hand*

Int. Journal of Integrated Engineering Vol. 17 No. 1 (2025) p. 401-415

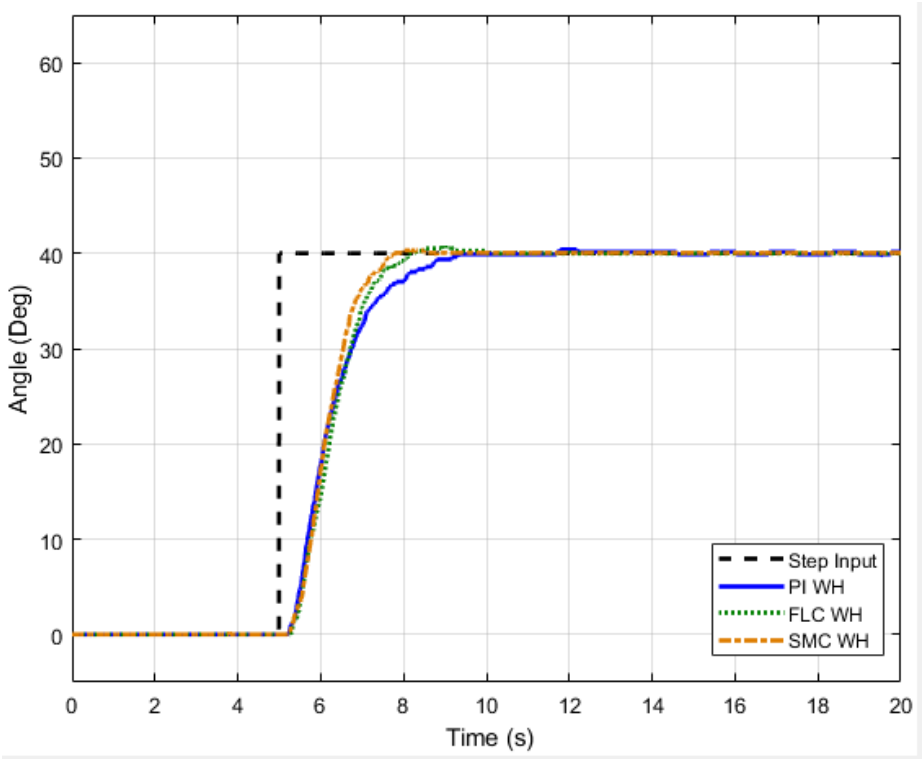

Fig. 13 *Graph output position for target angle 40° with the user's hand*

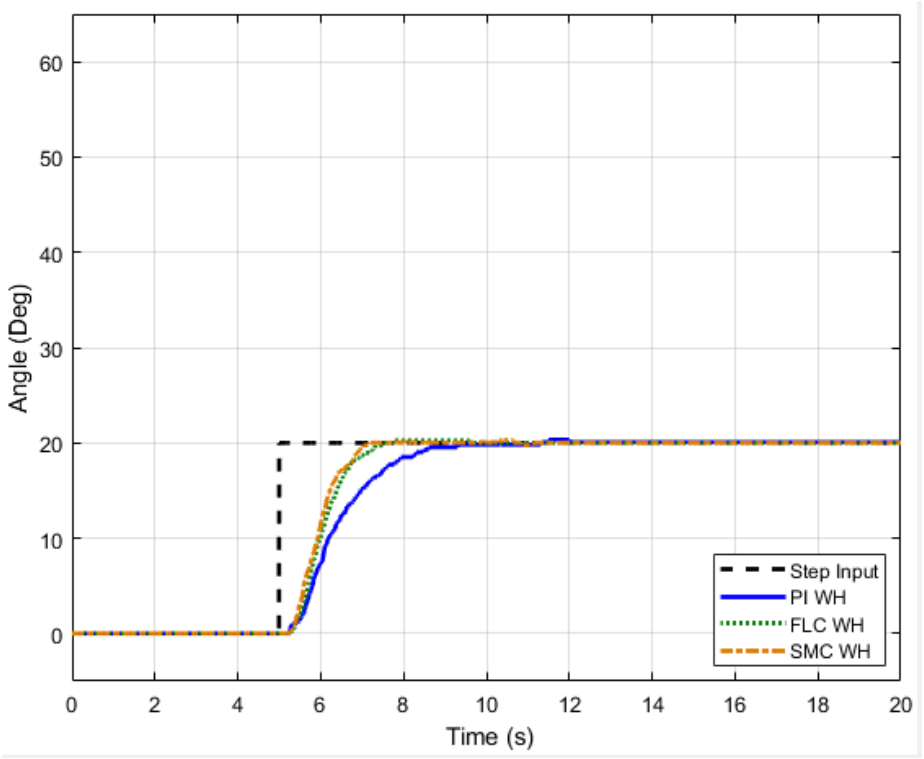

Fig. 14 *Graph output position for target angle 20° with the user's hand*

The results for the scenario in which the user wears the hand exoskeleton, targeting angles of 60°, 40°, and 20°, are illustrated in Fig. 12 to 14, respectively. Overall, all controllers successfully guide the hand exoskeleton to the desired target angles, demonstrating the device's effectiveness in assisting the user's hand movements, both in closing and opening the hand. This outcome highlights the exoskeleton's capability to enhance hand mobility and functionality.

Consistent with the scenarios where the user does not wear the exoskeleton, the Sliding Mode Controller (SMC) exhibits the fastest response to the target position across all angles, whereas the Proportional-Integral (PI) controller displays the slowest response. The SMC's rapid convergence to the target positions reinforces its suitability for applications requiring swift and precise movements, a critical factor in real-time control systems like hand exoskeletons.

Notably, when the user wears the exoskeleton, overshoot becomes evident in both the Fuzzy Logic Controller (FLC) and SMC responses. The FLC shows overshoot at all target angles, with peak angles reaching 60.25°, 40.77°, and 20.26° for target angles of 60°, 40°, and 20°, respectively. The SMC exhibits overshoot only at the 40° target angle, recording a peak angle of 40.31°. Despite the presence of overshoot, the deviations are minimal, with peak angles remaining within 1° of the target angles. These slight overshoots can be mitigated through gain adjustment for the FLC and an increase in the Delta parameter for the SMC, enhancing their precision.

In contrast, the PI controller consistently avoids overshoot across all target angles. However, the ripples observed in the PI controller's response when the user does not wear the exoskeleton persist even when the user wears the device. These ripples indicate residual oscillations that could affect long-term precision. Meanwhile, both the FLC and SMC maintain zero steady-state error, effectively handling disturbances introduced by the user's hand movements. This consistent performance underscores the robustness of the FLC and SMC in providing precise and stable control in dynamic environments, making them more reliable for applications where sustained accuracy is crucial. In conclusion, under conditions where the user is wearing the hand exoskeleton, the SMC emerges as the most effective control strategy. It offers the fastest response time coupled with high accuracy, establishing it as the optimal choice for ensuring precise and dependable control in hand exoskeleton systems.

Table 3 *Performance data for each controller*

Target angle	Condition	Controller	Percent overshoot (%OS)	Setting time, Ts (s)	Rise time, Tr (s)	Steady-state error, ess (°)
60°	Actual without user	PI	0	3.69	2.10	0.03
		FLC	0	3.15	2.03	0
		SMC	0	2.94	1.81	0
	Actual with user	PI	0	3.92	2.03	0.04
		FLC	0.41	3.45	2.04	0
		SMC	0	3.20	1.9	0
40°	Actual without user	PI	0	3.83	2.10	0.10
		FLC	0	2.5	1.50	0
		SMC	0	2.50	1.41	0
	Actual with user	PI	0	3.91	2.14	±0.14
		FLC	1.93	2.91	1.63	0
		SMC	0.78	2.55	1.43	0
20°	Actual without user	PI	0	4.93	2.22	0.18
		FLC	0	2.36	1.24	0
		SMC	0	1.90	1.12	0
	Actual with user	PI	0	4.31	2.30	0.07
		FLC	1.3	2.27	1.28	0
		SMC	0	2.04	1.33	0

Table 3 offers a detailed analysis of the performance metrics gathered from all conducted experiments, providing valuable insights into the efficacy of each controller. Notably, the PI controller consistently demonstrates zero overshoot across all experiments, while the FLC exhibits overshoot percentages of 0.41%, 1.93%, and 1.3% in experiments where the user wears the hand exoskeleton, targeting angles of 60°, 40°, and 20°, respectively. Conversely, SMC showcases overshoot solely in the experiment where the user wears the hand exoskeleton at a target angle of 40°, with a marginal value of 0.78%.

Across all target angles and conditions, SMC consistently displays the fastest settling and rise times, whereas the PI controller exhibits the slowest settling and rise times, except for scenarios where the user wears the hand

exoskeleton at a target angle of 60°, where the PI controller demonstrates a faster rise time compared to FLC. Notably, as the target angle decreases, both the settling and rise times decrease for SMC and FLC, whereas for the PI controller, the settling time remains relatively consistent regardless of the target angle, indicating a slower response as the target angle decreases.

Furthermore, both SMC and FLC demonstrate zero steady-state error across all conditions, indicating precise control over the angular position of the hand exoskeleton. In contrast, the PI controller exhibits a small but discernible steady-state error in all experiments, with values less than 0.2°, suggesting a minor deviation from the desired position in long-term operation.

Considering the experiment objectives, which prioritize minimal overshoot (%OS), negligible steady-state error (e), and rapid settling time (T_s), SMC emerges as the optimal controller for regulating the angular position of the shaft in the designed hand exoskeleton among the three controllers tested. This conclusion is bolstered by the minimal presence of overshoot in only one experiment, with a negligible value of 0.78%, combined with zero steady-state error and the fastest settling time observed across all experiments.

Conclusions

In conclusion, this study's findings highlight the superiority of Sliding Mode Control (SMC) in achieving stable and accurate position control for hand exoskeletons, particularly in the context of assisting stroke patients. The comparative analysis of controllers, including PI and Fuzzy Logic Control, highlights SMC's exceptional performance in minimizing overshoot, eliminating steady-state error, and achieving rapid settling time. These results have significant implications for advancing hand exoskeleton technology, enhancing rehabilitation outcomes, and improving industrial applications. By providing valuable insights into the effectiveness of different controllers, this research contributes to the ongoing development and implementation of control systems in hand exoskeleton technology. Through severe testing and analysis, it was found that while all three controllers demonstrated varying degrees of success in achieving precise position control, the SMC exhibited the most promising performance for this task. The SMC showed robustness against uncertainties and disturbances, providing stable and accurate control over the exoskeleton's movements. However, further research and experimentation may be warranted to explore the full potential of each controller and optimize their application in hand exoskeleton systems.

The contribution of this study lies in its comprehensive comparative analysis of three distinct controllers; Proportional Integral Derivative (PID), Fuzzy Logic Controller (FLC), and Sliding Mode Control (SMC), for regulating the position of the user's hand and fingers in hand exoskeletons. By systematically evaluating each controller's performance, this research provides valuable insights into their suitability for this specific task. The findings highlight the effectiveness of Sliding Mode Control (SMC) in achieving stable and accurate position control, particularly in the presence of uncertainties and disturbances. This contributes to advancing the field of exoskeleton technology by identifying a robust control strategy that can enhance the functionality and usability of such devices, ultimately benefiting individuals with hand impairments and other potential applications in rehabilitation and industrial tasks. In conclusion, these findings provide valuable guidance for the development and implementation of control systems in hand exoskeleton technology, with the potential to improve the quality of life for individuals with hand impairments and enhance applications in rehabilitation and industrial settings.

Acknowledgement

The authors would like to express their gratitude to the Ministry of Higher Education Malaysia and the Faculty of Electrical Technology and Engineering, Universiti Teknikal Malaysia Melaka (UTeM), for providing financial support under the IPTA Academic Training Scheme (SLAI), the Young Talent Researcher (YTR) Grant (600-RMC/YTR/5/3 (004/2021)) for financial assistance, and to the Faculty of Engineering Technology and the Faculty of Electrical and Electronic Engineering, Universiti Tun Hussein Onn Malaysia (UTHM), for providing a platform to carry out the research activities. This research was also financially supported by UTHM through the TIER1 Grant Scheme (Code Q487).

Conflict of Interest

Authors declare that there is no conflict of interests regarding the publication of the paper.

Author Contribution

The authors confirm their contribution to the paper as follows: ***study conception and design:*** *Ab Wafi Ab Aziz, Jamaludin Jalani, Amirul Syafiq Sadun;* ***data collection:*** *Ab Wafi Ab Aziz;* ***analysis and interpretation of results:*** *Ab Wafi Ab Aziz, Jamaludin Jalani;* ***draft manuscript preparation*** *Ab Wafi Ab Aziz, Jamaludin Jalani. All authors reviewed the results and approved the final version of the manuscript.*

References

[1] Du Plessis, T., Djouani, K., & Oosthuizen, C. (2021). A review of active hand exoskeletons for rehabilitation and assistance. *Robotics*, *10*(1). https://doi.org/10.3390/robotics10010040

[2] Sarac, M., Solazzi, M., & Frisoli, A. (2019). Design Requirements of Generic Hand Exoskeletons and Survey of Hand Exoskeletons for Rehabilitation, Assistive, or Haptic Use. *IEEE Transactions on Haptics*, *12*(4), 400–413. https://doi.org/10.1109/TOH.2019.2924881

[3] Y. Bleyenheuft, & Gordon, A. M. (2014). Precision grip in congenital and acquired hemiparesis: Similarities in impairments and implications for neurorehabilitatio. *Frontiers in Human Neuroscience*, *8*(JUNE), 1–11. https://doi.org/10.3389/fnhum.2014.00459

[4] Ferguson, P. W., Shen, Y., & Rosen, J. (2019). Hand exoskeleton systems-overview. In *Wearable Robotics: Systems and Applications*. INC. https://doi.org/10.1016/B978-0-12-814659-0.00008-4

[5] Tiboni, M., Borboni, A., Vérité, F., Bregoli, C., & Amici, C. (2022). Sensors and Actuation Technologies in Exoskeletons: A Review. *Sensors*, *22*(3), 1–61. https://doi.org/ 10.3390/s22030884

[6] Hays, E., Slayton, J., Tejeda-Godinez, G., Carney, E., Cruz, K., Exley, T., & Jafari, A. (2023). A Review of Rehabilitative and Assistive Technologies for Upper-Body Exoskeletal Devices. *Actuators*, *12*(4). https://doi.org/ 10.3390/act12040178

[7] Anandan, K., Rajagopalan, N., Mohanavelu, & Mary, S. (2023). Design And Development Of Biosignal Controlled Hand Exoskeleton For Assistive Purposes. *Journal of Mechanics in Medicine and Biology*, *23*(06), 2340033. https://doi.org/ 10.1142/S021951942340033X

[8] Ab Aziz, A. W., Jalani, J., Sadun, A. S., & Hussin, M. Z. (2024). A Low Cost of an Exoskeleton Finger for Stroke Patient. *Journal of Advanced Research in Applied Sciences and Engineering Technology*, *38*(2), 16–26. https://doi.org/10.37934/araset.38.2.1626

[9] Qi, W., Sun, S., Niu, T., & Zhao, D. (2024). Research and prospects of virtual reality systems applying exoskeleton technology. *Universal Access in the Information Society*, *23*(1), 119–140. https://doi.org/10.1007/s10209-022-00929-0

[10] Bartalucci, L., Secciani, N., Brogi, C., Topini, A., Della Valle, A., Ridolfi, A., & Allotta, B. (2023). An original mechatronic design of a kinaesthetic hand exoskeleton for virtual reality-based applications. *Mechatronics*, *90*, 102947. https://doi.org/10.1016/j.mechatronics.2023.102947

[11] Akgun, G., Cetin, A. E., & Kaplanoglu, E. (2020). Exoskeleton design and adaptive compliance control for hand rehabilitation. *Transactions of the Institute of Measurement and Control*, *42*(3), 493–502. https://doi.org/10.1177/0142331219874976

[12] Roshdy, A., Al Kork, S., Said, S., & Beyrouthy, T. (2019). A wearable exoskeleton rehabilitation device for paralysis - A comprehensive study. *Advances in Science, Technology and Engineering Systems*, *4*(1), 17–26. https://doi.org/10.25046/aj040103

[13] Ou, Y. K., Wang, Y. L., Chang, H. C., & Chen, C. C. (2020). Design and development of a wearable exoskeleton system for stroke rehabilitation. *Healthcare (Switzerland)*, *8*(1), 1–14. https://doi.org/10.3390/healthcare8010018

[14] Hernández-Santos, C., Davizón, Y. A., Said, A. R., Soto, R., Felix-Herrán, L. C., & Vargas-Martínez, A. (2021). Development of a wearable finger exoskeleton for rehabilitation. *Applied Sciences (Switzerland)*, *11*(9), 1–17. https://doi.org/10.3390/app11094145

[15] Secciani, N., Bianchi, M., Ridolfi, A., Vannetti, F., Volpe, Y., Governi, L., Bianchini, M., & Allotta, B. (2019). Tailor-made hand exoskeletons at the university of florence: From kinematics to mechatronic design. *Machines*, *7*(2), 1–18. https://doi.org/10.3390/machines7020022

[16] Popov, D., Gaponov, I., & Ryu, J. H. (2017). Portable exoskeleton glove with soft structure for hand assistance in activities of daily living. *IEEE/ASME Transactions on Mechatronics*, *22*(2), 865–875. https://doi.org/10.1109/TMECH.2016.2641932

[17] Marconi, D., Baldoni, A., McKinney, Z., Cempini, M., Crea, S., & Vitiello, N. (2019). A novel hand exoskeleton with series elastic actuation for modulated torque transfer. *Mechatronics*, *61*(November 2018), 69–82. https://doi.org/10.1016/j.mechatronics.2019.06.001

[18] Topini, A., Sansom, W., Secciani, N., Bartalucci, L., Ridolfi, A., & Allotta, B. (2022). Variable Admittance Control of a Hand Exoskeleton for Virtual Reality-Based Rehabilitation Tasks. *Frontiers in Neurorobotics*, *15*(January), 1–18. https://doi.org/10.3389/fnbot.2021.789743

[19] De la Cruz-Sánchez, B. A., Arias-Montiel, M., & Lugo-González, E. (2022). EMG-controlled hand exoskeleton for assisted bilateral rehabilitation. *Biocybernetics and Biomedical Engineering*, *42*(2), 596–614. https://doi.org/10.1016/j.bbe.2022.04.001

[20] Vangi, M., Brogi, C., Topini, A., Secciani, N., & Ridolfi, A. (2023). Enhancing sEMG-Based Finger Motion Prediction with CNN-LSTM Regressors for Controlling a Hand Exoskeleton. *Machines*, *11*(7). https://doi.org/10.3390/machines11070747

[21] Esmatloo, P., & Deshpande, A. D. (2020). Fingertip position and force control for dexterous manipulation through model-based control of hand-exoskeleton-environment. *IEEE/ASME International Conference on Advanced Intelligent Mechatronics, AIM*, *2020-July*, 994–1001. https://doi.org/10.1109/AIM43001.2020.9158879
[22] Cui, H., Lai, B., & Zheng, Q. (2022). Multimodal motion analysis in the finger exoskeleton rehabilitation exercise. *Proc.SPIE*, *12457*, 1245717. https://doi.org/10.1117/12.2660835
[23] Kumar, G., Kumar, R., & Kumar, A. (2023). A Review of the Controllers for Structural Control. *Archives of Computational Methods in Engineering*, *30*(6), 3977–4000. https://doi.org/10.1007/s11831-023-09931-y
[24] Rekha Yoganathan Jamuna Venkatesan, T. V. N., & Christopher, I. W. (2024). Performance Comparison of a DC–DC Boost Converter With Conventional and Non-linear SMC Controller in Dual Loop Structure. *Electric Power Components and Systems*, *0*(0), 1–16. https://doi.org/10.1080/15325008.2024.2340744
[25] Rekha, Y., Jamuna, V., & Christopher, I. W. (2023). Cascaded Inner Loop Fuzzy SMC for DC–DC Boost Converter. *Journal of Circuits, Systems and Computers*, *32*(16), 2350269. https://doi.org/10.1142/S0218126623502699
[26] Rahmatullah, R., Ak, A., & serteller, N. F. O. (2023). SMC Controller Design for DC Motor Speed Control Applications and Performance Comparison with FLC, PID and PI Controllers. In A. K. Nagar, D. Singh Jat, D. K. Mishra, & A. Joshi (Eds.), *Intelligent Sustainable Systems* (pp. 607–617). Springer Nature Singapore. https://doi.org/10.1007/978-981-19-7663-6_57
[27] Ananthi, K., & Manoharan, S. (2022). Performance Analysis of Effective Controller for Active Power Filter using PUC5 Inverter for Improving Power Quality. *Journal of Electrical Engineering and Technology*, *17*(4), 2107–2121. https://doi.org/ 10.1007/s42835-022-01039-w
[28] Esposito, D., Centracchio, J., Andreozzi, E., Savino, S., Gargiulo, G. D., Naik, G. R., & Bifulco, P. (2022). Design of a 3D-Printed Hand Exoskeleton Based on Force-Myography Control for Assistance and Rehabilitation. *Machines*, *10*(1), 57. https://doi.org/10.3390/machines10010057
[29] Wen, S. H., Zheng, W., Jia, S. D., Ji, Z. X., Hao, P. C., & Lam, H. K. (2020). Unactuated Force Control of 5-DOF Parallel Robot Based on Fuzzy PI. *International Journal of Control, Automation and Systems*, *18*(6), 1629–1641. https://doi.org/10.1007/s12555-018-0579-7
[30] Sharma, R., Gaur, P., Bhatt, S., & Joshi, D. (2021). Optimal fuzzy logic-based control strategy for lower limb rehabilitation exoskeleton. *Applied Soft Computing*, *105*, 107226. https://doi.org/10.1016/j.asoc.2021.107226
[31] Wu, Q., Wang, X., Du, F., & Xi, R. (2017). Modeling and position control of a therapeutic exoskeleton targeting upper extremity rehabilitation. *Proceedings of the Institution of Mechanical Engineers, Part C: Journal of Mechanical Engineering Science*, *231*(23), 4360–4373. https://doi.org/10.1177/0954406216668204
[32] Zhao, W., & Song, A. (2020). Active motion control of a knee exoskeleton driven by antagonistic pneumatic muscle actuators. *Actuators*, *9*(4), 1–14. https://doi.org/10.3390/act9040134
[33] Kiss, J. M., Szemes, P. T., & Aradi, P. (2021). Sliding mode control of a servo system in LabVIEW: Comparing different control methods. *International Review of Applied Sciences and Engineering*, *12*(2), 201–210. https://doi.org/10.1556/1848.2021.00250
[34] Neubauer, M., Brenner, F., Hinze, C., & Verl, A. (2021). Cascaded sliding mode position control (SMC-PI) for an improved dynamic behavior of elastic feed drives. *International Journal of Machine Tools and Manufacture*, *169*(July), 103796. https://doi.org/10.1016/j.ijmachtools.2021.103796
[35] Dhiman, D. J. S. K. S. P. (2022). Comparative Analysis of Defuzzification Techniques for Fuzzy Output. *Journal of Algebraic Statistics*, *13*(2), 874–882. https://publishoa.com
[36] Berbaoui, B., Benachaiba, C., Dehini, R., & Ferdi, B. (2010). Optimization of shunt active power filter system fuzzy logic controller based on ant colony algorithm. *Journal of Theoretical and Applied Information Technology*, *14*(2), 117–125.
[37] Mitra, P., Dey, C., & Mudi, R. K. (2021). Fuzzy rule-based set point weighting for fuzzy PID controller. In *SN Applied Sciences* (Vol. 3, Issue 6). https://doi.org/10.1007/s42452-021-04626-0
[38] Chen, C. T., Lien, W. Y., Chen, C. T., & Wu, Y. C. (2020). Implementation of an upper-limb exoskeleton robot driven by pneumatic muscle actuators for rehabilitation. *Actuators*, *9*(4), 1–19. https://doi.org/10.3390/act9040106